Electronic Supplementary Material (ESI) for Nanoscale.

Supporting Information for

Plasmonic ELISA Based on Controlled Growth of Silver Nanoparticles

Zhihong Xuan,[a] Mingmin Li,[a] Pengfei Rong,[c] Wei Wang,[c] Yijun Li,[,a] Dingbin Liu[*,a,b]*

[a]*College of Chemistry, Research Center for Analytical Sciences, State Key Laboratory of Medicinal Chemical Biology, and Tianjin Key Laboratory of Molecular Recognition and Biosensing, Nankai University, Tianjin 300071, China.*

[b]*Collaborative Innovation Center of Chemical Science and Engineering (Tianjin), Tianjin 300071, China.*

[c]*Department of Radiology, The Third Xiangya Hospital, Central South University, Changsha, Hunan 410013, China.*

Contents

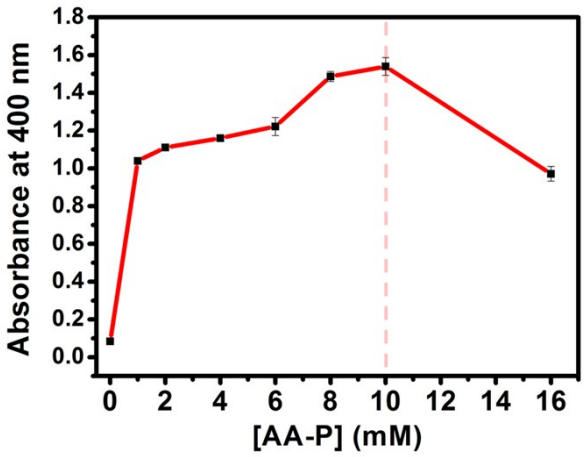

Figure S1. Effect of AA-P concentrations on the growth of AgNPs. 10 U/L ALP, 160 mM DEA buffer, and 30 mM $AgNO_3$ were used in this study. Error bars show the standard deviations of three independent measurements.

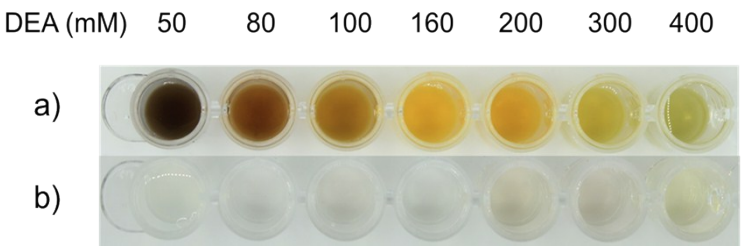

Figure S2. Effect of DEA concentrations on the growth of AgNPs. Photographs of the obtained AgNPs dispersed in DEA buffer with various concentrations, pretreated with 10 mM AA-P and 30 mM $AgNO_3$ in the presence (a) and absence (b) of 10 U/L ALP.

Table S1. A comparison of colorimetric assays for sensing ALP.

Material	Approach	Readout	Naked-eye	LOD	Ref
AuNPs	Click chemistry-triggered nanoparticle aggregation	Colorimetry	5 U/L	0.2 U/L	1
AuNRs	Silver nanoshell deposition on AuNR	Colorimetry	20 U/L	3.3 U/L	2
AuNPs	charge-induced nanoparticle aggregation	Colorimetry	-	1.7 μM	3
AuNPs	non-crosslinking nanoparticle aggregation	Colorimetry	-	8 U/mL	4
AuNPs	charge-induced nanoparticle aggregation	Colorimetry	-	10 U/L	5
AuNRs	etching of AuNRs	Colorimetry	0.2 U/L	0.01 U/L	6
Au NPs	Silver deposition on the surface of AuNPs	Colorimetry	-	12fM ~ 1.2×10^{-5} U/mL	7
AgNPs	ALP-mediated AgNP growth	Colorimetry	0.5 U/L	0.03 U/L	This study

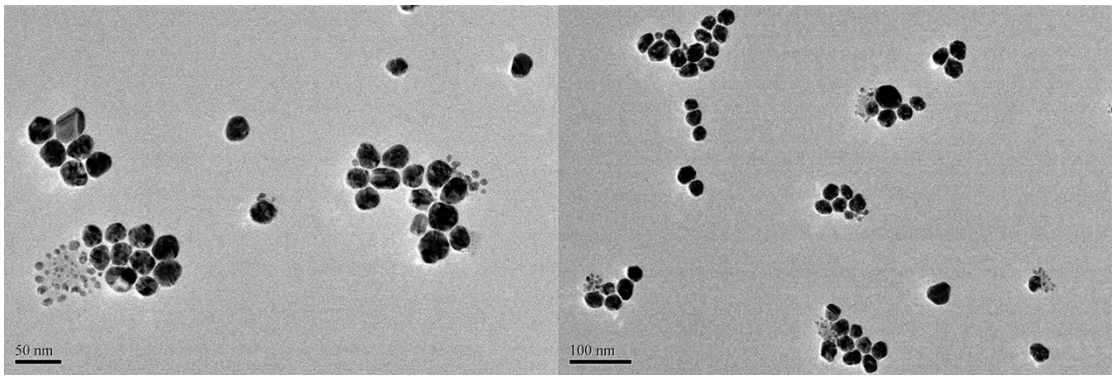

Figure S3. TEM images of AgNPs obtained with the mixing of 5 U/L of ALP, 10 mM AA-P, and 30 mM $AgNO_3$. Scale bars: 50 nm (left) and 100 nm (right).

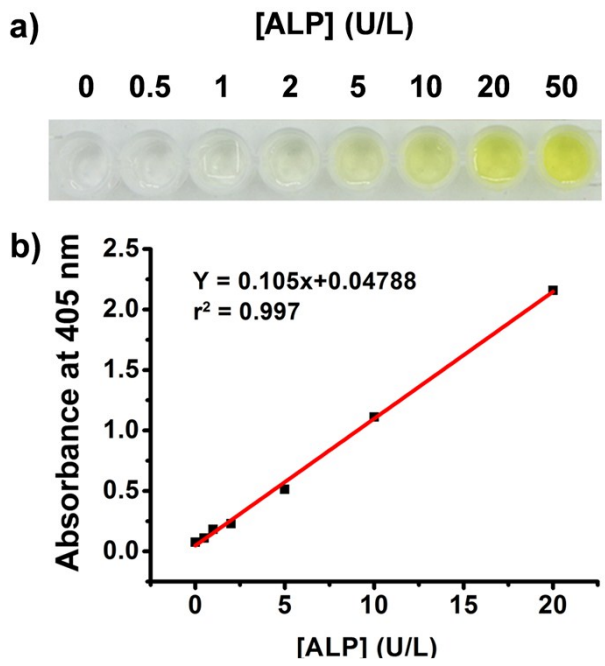

Figure S4. Detection of ALP activity using the classical pNPP-based assay. a) Naked-eye results of ALP detection with various concentrations ranging from 0 to 50 U/L. b) The absorbance of the pNPP products at 405 nm plotting the concentrations of ALP in a).

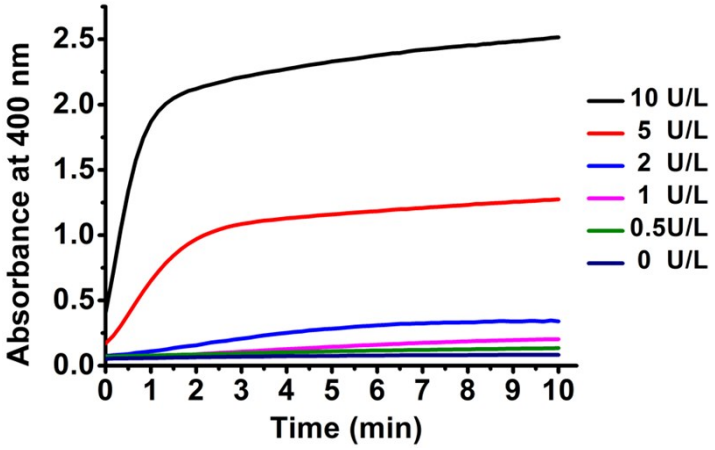

Figure S5. The dynamic process of the AgNPs growth at various concentrations of ALP from 0-10 U/L.

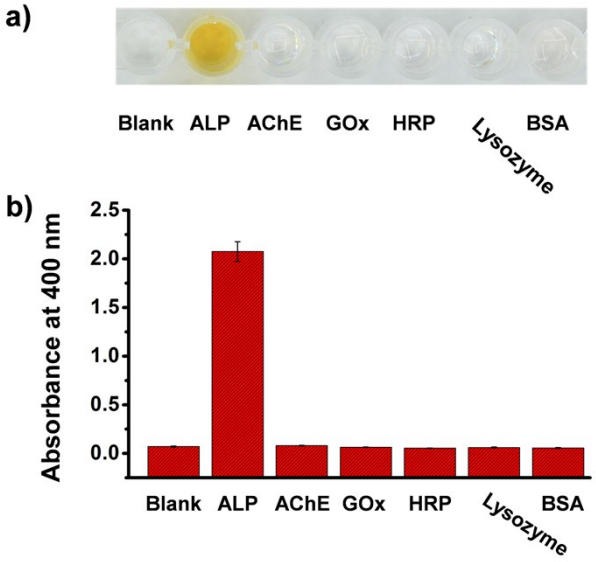

Figure S6. The specificity investigation of the AgNP-based plasmonic assay by incubating AA-P (10 mM) with ALP and a panel of other enzymes with the same concentration (10 U/L) and 1 mg/mL of BSA, followed by adding 30 mM of $AgNO_3$.

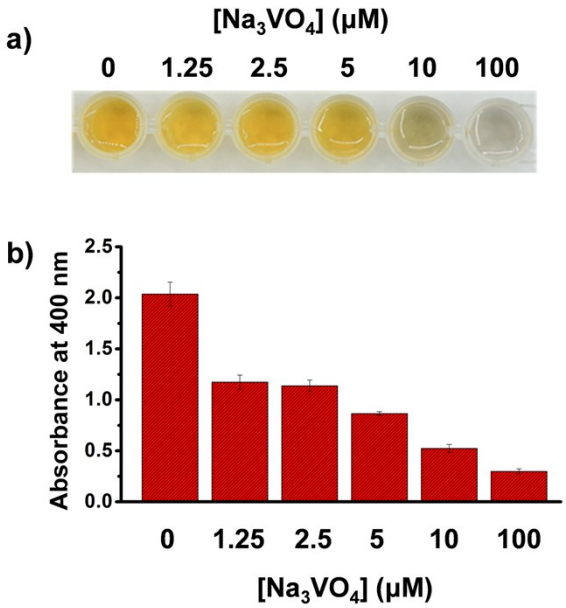

Figure S7. Enzyme inhibitor investigation by treating ALP (10 U/L) with various concentrations of Na_3VO_4 (0-100 μM), followed by adding AA-P (10 mM) and incubated at 37 °C for 1 h, then $AgNO_3$ (30 mM) was added to the obtained solutions.

Table S2. Optimizing the concentration of biotinylated detection antibody.

[AFP] (ng/mL)	100					0				
[SA-ALP] (μg/mL)	1									
[biotin-Ab2] (ng/mL)	0.5	1	1.5	2	4	0.5	1	1.5	2	4
$\bar{A}_{400\ nm}$	0.41	0.79	0.93	1.15	1.24	0.073	0.089	0.095	0.136	0.176

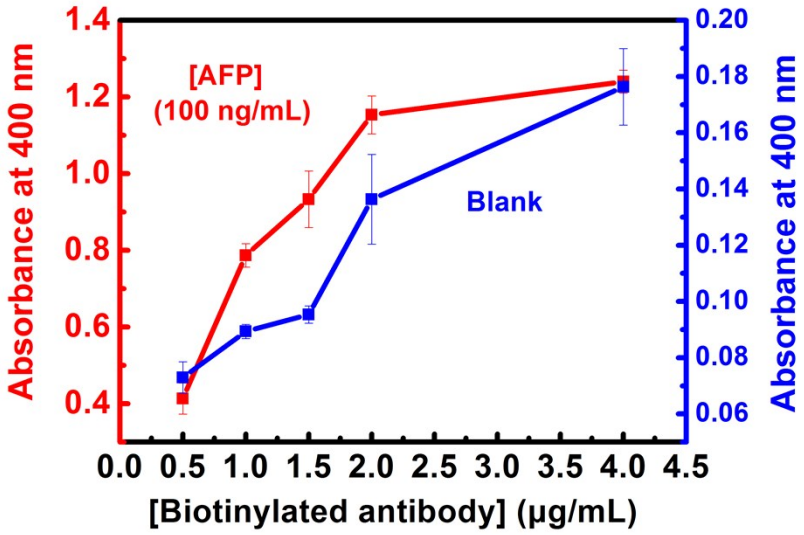

Figure S8. Optimizing the concentration of biotinylated detection antibody (the concentration of AFP is 100 ng/mL; the concentration of SA-ALP is 1 μg/mL). The absence of AFP was employed as the blank.

Table S3. Optimizing the concentration of SA-ALP.

[AFP] (ng/mL)	100					0				
[biotin-Ab2] (μg/mL)	2									
[SA-ALP] (μg/mL)	0.5	0.8	1	0.5	2	0.5	0.8	1	0.5	2
$\bar{A}_{400\ nm}$	0.45	0.82	0.99	1.2	1.57	0.074	0.092	0.097	0.194	0.303

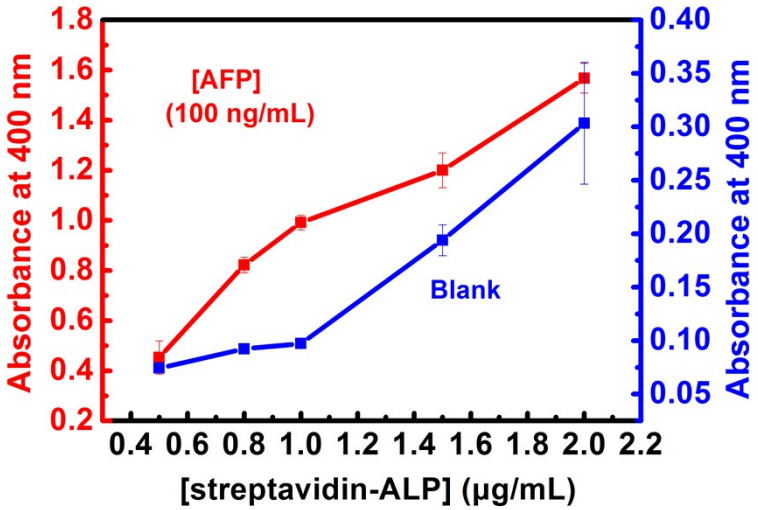

Figure S9. Optimizing the concentration of SA-ALP (the concentration of AFP is 100 ng/mL; the concentration of biotin-Ab2 is 2 μg/mL). The absence of AFP was employed as the blank.

Table S4. Detailed Information of the 54 serum samples collected from different people and the absorbance at 400 nm or 450 nm using the plasmonic ELISA and the HRP-based ELISA. (F and M are the abbreviation of female and male, respectively)

Plates No.	Supplied by hospital				Plasmonic ELISA		HRP-based ELISA	
	Serum No.	Age (year)	Gender	Cancer type	OD 400 nm	AFP positive or negative	OD 450nm	AFP positive or negative
A1	30	46	F	Normal	0.29	Positive	0.066	Negative
A2	29	46	F	Normal	0.418	Positive	0.081	Negative
A3	9	60	M	Normal	0.808	Positive	0.076	Negative
A4	493	78	M	Lung cancer	0.346	Positive	0.112	Negative
A5	282	65	M	Colon cancer	0.358	Positive	0.08	Negative
A6	109	46	M	Rectal cancer	0.265	Positive	0.091	Negative
A7	151	37	F	Gastric cancer	> 4	Positive	> 4	Positive
A8	111	45	M	Liver cancer	> 4	Positive	> 4	Positive
A9	447	57	M	Liver cancer	> 4	Positive	> 4	Positive
B1	265	77	F	Rectal cancer	0.71	Positive	0.073	Negative
B2	10	51	F	Normal	0.315	Positive	0.074	Negative
B3	93	41	M	Uncertain	1.006	Positive	0.307	Positive
B4	442	48	M	Lung cancer	0.376	Positive	0.085	Negative
B5	184	71	M	Colon cancer	0.704	Positive	0.082	Negative
B6	118	56	F	Breast cancer	0.397	Positive	0.074	Negative
B7	183	58	F	Colon cancer	0.724	Positive	0.118	Negative
B8	422	73	M	Lung cancer	0.452	Positive	0.099	Negative
B9	144	58	F	Lung cancer	0.409	Positive	0.114	Negative
C1	363	74	M	Normal	0.331	Positive	0.081	Negative
C2	75	40	M	Uncertain	> 4	Positive	> 4	Positive
C3	364	80	M	Normal	0.273	Positive	0.083	Negative
C4	429	68	M	Gastric cancer	0.311	Positive	0.085	Negative
C5	508	66	M	Gastric cancer	1.073	Positive	0.094	Negative
C6	119	64	M	Lung cancer	0.298	Positive	0.077	Negative
C7	108	62	M	Liver cancer	1.739	Positive	0.53	Positive
C8	150	59	M	Bile duct cancer	0.346	Positive	0.107	Negative
C9	552	33	M	Liver cancer	> 4	Positive	> 4	Positive
D1	311	57	F	Normal	0.519	Positive	0.082	Negative
D2	322	50	F	Normal	0.121	Negative	0.077	Negative
D3	314	76	M	Normal	0.271	Positive	0.082	Negative
D4	172	29	F	Normal	0.636	Positive	0.098	Negative
D5	130	60	F	Breast cancer	0.927	Positive	0.083	Negative
D6	120	Unknown	Unknown	Normal	0.528	Positive	0.08	Negative
D7	362	37	F	Colon cancer	0.293	Positive	0.351	Negative
D8	307	75	M	Liver cancer	0.983	Positive	0.3	Positive
D9	349	50	M	Colon cancer	0.34	Positive	0.092	Negative
E1	366	Unknown	Unknown	Uncertain	0.997	Positive	0.076	Negative
E2	316	80	M	Normal	0.598	Positive	0.079	Negative
E3	20	41	F	normal	0.424	Positive	0.083	Negative
E4	415	67	M	gastric cancer	0.482	Positive	0.081	Negative
E5	110	46	M	Uncertain	0.407	Positive	0.089	Negative
E6	121	51	M	lung cancer	0.372	Positive	0.081	Negative
E7	533	56	M	Lung cancer	0.457	Positive	0.09	Negative
E8	194	62	M	Lung cancer	0.757	Positive	0.09	Negative
E9	563	66	F	liver cancer	> 4	Positive	> 4	Positive
F1	19	Unknown	Unknown	Normal	0.324	Positive	0.07	Negative
F2	180	65	F	Rectal cancer	0.393	Positive	0.074	Negative
F3	546	86	F	Uncertain	> 4	Positive	> 4	Positive
F4	140	67	M	Lung cancer	0.474	Positive	0.078	Negative
F5	158	68	F	Normal	0.598	Positive	0.077	Negative
F6	576	49	F	Rectal cancer	0.416	Positive	0.075	Negative
F7	439	49	M	Lung cancer	0.344	Positive	0.105	Negative
F8	273	72	M	Osteosarcoma	0.387	Positive	0.042	Negative
F9	92	49	M	Liver cancer	> 4	Positive	> 4	Positive

Table S5. The statistical number of the different cancer types among the 54 serum samples.

Cancer type	Liver cancer	Gastric cancer	Lung cancer	Colon cancer	Rectal cancer	Breast cancer	Osteos arcoma	Bile duct cancer	Normal	Uncertain	Sum
Number	7	4	10	5	4	2	1	1	15	5	54

Table S6. The detail information of the 7 samples experienced therapeutics and the absorbance at 400 nm or 450 nm using the plasmonic ELISA and the HRP-based ELISA. (F and M are the abbreviation of female and male, respectively)

Plates No.	Supplied by hospital				Plasmonic ELISA		HRP-based ELISA	
	Serum No.	Age (year)	Gender	Cancer types & Treatment protocols or Results	OD 400 nm	AFP positive or negative	OD 450nm	AFP positive or negative
1	20	41	F	Hepatocellular carcinoma after interventional therapy	> 4	Positive	> 4	Positive
2	95	67	M	Hepatocellular carcinoma after interventional therapy	1.469	Positive	0.13	Negative
3	125	48	M	Large area of lung cancer metastasis and then chemotherapy	0.421	Positive	0.121	Negative
4	416	50	F	Lung cancer after treatment	0.685	Positive	0.12	Negative
5	424	51	F	Sigmoid colon cancer after postoperative and chemotherapy	0.365	Positive	0.112	Negative
6	458	66	M	Hepatic metastasis of colonic carcinoma and then chemotherapy	0.416	Positive	0.12	Negative
7	475	58	F	Multiple transfer of colon cancer and then chemotherapy	0.946	Positive	0.12	Negative

Supplementary Methods

The detailed procedures for controlling the ALP-mediated growth of AgNPs. The most effective working pH and incubation temperature for ALP activity are 9.8 and 37 °C respectively.[2] Under these conditions, other experimental parameters including AA-P concentration, $AgNO_3$ concentration, DEA concentration were carefully investigated since they are sensitive to the growth of AgNPs. As shown in Figure S1, the absorbance at 400 nm of the obtained AgNPs increased when AA-P concentrations increased from 0 to 10 mM but then decreased from 10 to 16 mM. It is reasonable that higher concentrations of AA-P may produce more AA, thus catalyzing the formation

of more AgNPs. However, higher concentrations of AA-P could make the formed AgNPs aggregate within a few minutes, which is likely attributed to the high concentrations of salts in the obtained AgNPs solutions. Thus, the optimal concentration of AA-P here is 10 mM.

To ensure the oxidation-reduction reaction between AA and $AgNO_3$ proceeds rapidly and AA can be consumed as much as possible, excess $AgNO_3$ (30 mM) should be added to the mixtures.

DEA buffer at pH 9.8 offers the alkaline environment for the catalytic hydrolysis of ALP toward AA-P. The concentration of the DEA buffer used in this study is vital for the growth of AgNPs. Lower (50-100 mM) or higher (300-400 mM) concentration of DEA buffer neither obtained settled solution until the concentration is at suitable values (160-200 mM) (Figure S3a). According to the previous report,[6] DEA buffer is crucial for preventing the formation of the silver hydroxide precipitates under alkaline conditions. Therefore, the muddy brown solutions obtained in 50-100 mM DEA buffers can be attributed to the formation of silver hydroxide precipitate. The reason why higher concentrations of DEA buffer (300-400 mM) lead to slightly dark yellow solution is still unknown (Figure S2a). Nonetheless, higher concentrations of DEA buffer could also result in the self-hydrolysis of AA-P (Figure S2b), thus may induce background noise even in the absence of detection targets. In order to avoid the presence of the silver hydroxide precipitate and the self-hydrolysis of AA-P, 160 mM of DEA buffer was used throughout this study.

Taken together, the optimal concentrations of AA-P, $AgNO_3$, and DEA buffer are 10 mM, 30 mM, and 160 mM respectively.

Conjugation of NHS-activated biotin to detection antibodies. NHS-activated biotin was dissolved in dry DMSO before diluting in final reaction buffer. Detection antibodies (Ab2) were prepared in 100 μL of PBS (pH 7.4) at a concentration of 1.0 mg/mL. Then, the NHS-biotin (6 mM, 3 μL) was mixed with the Ab2 solution at a 30:1 mole ratio and incubated at room temperature for 4 h with mild concussion. The reaction was stopped by adding quenching buffer (1 M Tris-HCl, pH 8) to a final concentration of 50 mM Tris and allowing the quenching reaction to proceed at room temperature for 5 min. The resulting products were purified by using a centrifugal filter device (Amicon Ultra-0.5, Millipore) with a 30K Nominal Molecular Weight Limit (NMWL).

The experimental details for conjugating ALP with detection antibodies. To avoid the false positive signals produced by nonspecific adsorption of the biotinylated antibody (biotin-Ab2) or the SA-ALP, their concentrations for fabricating the plasmonic ELISA were investigated. Various concentrations of biotin-Ab2 from 0.5 to 4 μg/mL were incubated with aliquots of 100 ng/mL AFP and 1 μg/mL of SA-ALP in the capture antibody-immobilized wells, respectively (Table S2). As depicted in Figure S8, the absorbance at 400 nm intensified as the concentration of biotin-Ab2 increased. When the concentrations increased to be 2 and 4 μg/mL, the maximal absorbance can be achieved. In contrast, the absence of AFP induce a negligible increase of absorbance for lower concentrations of biotin-Ab2. However, false-positive signals can be observed when the concentrations of biotin-Ab2 increased up to 2 μg/mL. Therefore, to avoid false positive signals in blank wells and to obtain strong specific signals simultaneously, 2 μg/mL of biotin-Ab2 is chosen in this study. In addition, the concentration of SA-ALP was optimized to be 1 μg/mL by the same principle (Table S3, Figure S9).

Procedures for HRP-based ELISA. We performed the detection procedures strictly by following the recommended steps as received. Briefly, 100 μL of different concentrations of AFP standard solutions were added to the capture antibody-coated microplates and incubated at 37 °C for 20 min. After incubation, the wells were washed three times with washing buffer. Then, 100 μL of HRP-linked antibodies were added to each well and incubated at 37 °C for 15 min. Following the same washing steps, 50 μL chromogenic A and 50 μL chromogenic B were added to the plate successively and then the plate was standing at room temperature for 5 min. At last, 50 μL stop solution was added to stop the catalytic process and the optical density at the wavelength of 450 nm was detected by a Synergy 2 Multi-Mode Microplate Reader.

The serum samples were also measured by a commercial HRP-based ELISA kit. The procedure is the same as that for the AFP standard solutions except that the 100 μL AFP standard solution was replaced by 50 μL serum.

References

1. Y. Xianyu, Z. Wang and X. Jiang, *ACS. Nano*, 2014, **8**, 12741-12747.

2. Z. Gao, K. Deng, X.-D. Wang, M. Miró and D. Tang, *ACS Appl. Mater. Interfaces*, 2014, **6**,

18243-18250.

3. Y. Choi, N. H. Ho and C. H. Tung, *Angew. Chem. Int. Ed*, 2007, **46**, 707-709.

4. W. Zhao, W. Chiuman, J. C. Lam, M. A. Brook and Y. Li, *Chem. Commun*, 2007, 3729-3731.

5. C. M. Li, S. J. Zhen, J. Wang, Y. F. Li and C. Z. Huang, *Biosens. Bioelectron*, 2013, **43**, 366-371.

6. Z. Zhang, Z. Chen, S. Wang, F. Cheng and L. Chen, *ACS Appl. Mater. Interfaces*, 2015, **7**, 27639-27645.

7. C. H. Zhou, J. Y. Zhao, D. W. Pang and Z. L. Zhang, *Anal. Chem*, 2014, **86**, 2752-2759.